Pseudosymmetry and Chiral Discrimination in Optical Resolution *via* Diastereoisomeric Salt Formation. The Crystal Structures of (*R*)- and (*S*)-*N*-Methylamphetamine Bitartrates (RMERTA and SMERTA)

Elemér Fogassy, Mária Ács, and Ferenc Faigl
Department of Organic Chemical Technology, Technical University, Budapest, H-1521 Hungary
Kálmán Simon,* János Rohonczy, and Zoltán Ecsery
Chinoin Research Centre, Budapest POB 110, H-1325 Hungary

The structures of the diastereoisomeric salts of (*R*)- and (*S*)-*N*-methylamphetamine bitartrates (RMERTA and SMERTA) have been determined by *X*-ray crystallography. Comparison of these crystal structures provides an insight into the mechanism of optical resolution *via* diastereoisomeric salt formation. The very small difference between the two crystal structures indicates that specific interactions such as CH • • • O interactions may play an important role in molecular recognition.

Since Pasteur, the problems of optical resolution have remained unsolved. Despite the practical importance of the technique, the structural basis of resolution and the role of thermodynamic and kinetic factors during optical resolution *via* diastereoisomeric salt formation are not known.

We have studied a series of optical resolutions *via* diastereoisomeric salt formation and found a correlation between the optical yield (optical purity × chemical yield) and the electronic parameters of the substituents attached to the chiral centre.[1,2] Our model fits the experimental results well, but appreciation of the interactions causing chiral discrimination may be enhanced by studying a given diastereoisomer salt pair. A possible method for the determination of second-order interactions is *X*-ray crystallography.

As a model we have chosen the optical resolution of *N*-methylamphetamine (an intermediate of the synthetic anti-Parkinson agent[3] JUMEX®) with (*RR*)-tartaric acid in ethanol (Scheme). Although tartaric acid is widely used as a resolving agent, there are only a few examples where the crystal structures of both diastereoisomeric salts are known. Some authors have attempted to find differences in the hydrogen-bonding systems of the salts to explain the separability of diastereoisomeric salts. Larsen found a similar hydrogen-bonding pattern for two pairs of substituted ammonium bitartrates, and came to the conclusion that non-bonded interactions of an undisclosed nature might account for the energy difference between the two diastereoisomers.[4,5]

Kuramoto *et al.* studied the structures and thermal behaviour of diastereoisomeric salts of Co^{III} complexes with tartaric acid,[6] and concluded that the bitartrate chain plays an important role in the discrimination of the enantiomers.

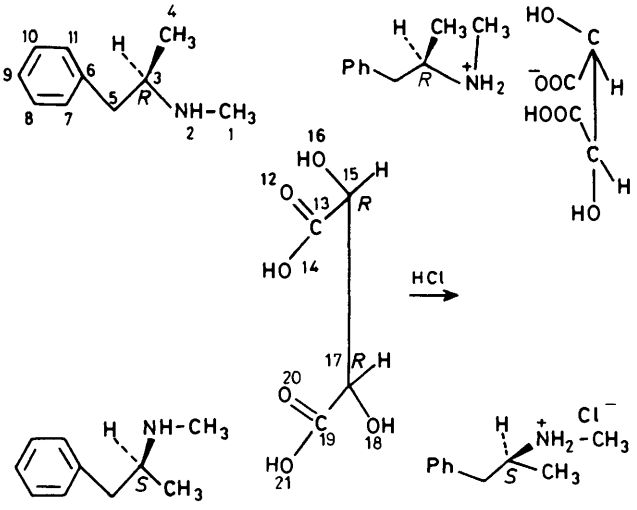

Scheme.

Results and Discussion

From a survey of the bitartrate structures available in the Cambridge Crystallographic Database (Table 1, references in Table 2), we came to the conclusion that tartaric acid in its acidic salts forms a head-to-tail-type bitartrate chain, linked by a strong hydrogen-bond system, independently of the nature of the cation (chiral or achiral). In all but three cases the carboxy hydroxy is antiperiplanar with the vicinal hydroxy. In the BIKZOK10 and TRHTRT structures the deviation from 180° is quite large; this is probably due to the fact that two hydrogen bonds are present between neighbouring counterions, resulting in conformational distortions. The carbon chain is antiperiplanar in all cases. The inclination angle between the two halves of the molecule is *ca.* 60°. It is worth mentioning that at least one 2_1 axis is present in all structures. The head-to-tail-type hydrogen-bonding is a general feature of these structure, determining the lattice parameters in one direction (7.05—7.83 Å).

In order to find some connection between the crystal structure and the results of resolution, we have studied the diastereoisomeric salts obtained during the resolution of our model (Scheme) in ethanol.[7]

The crystal data (Table 3) reveal that the cell dimensions of the diastereoisomeric salts are similar, but the crystal density of the *R*-base salt (RMERTA) is higher than that of the *S*-base salt (SMERTA). The conformations of the corresponding ions are similar (Table 4). In the cation the two methyl groups [C(1) and C(4)] are gauche, while N–C–C–C_{Phe} is antiperiplanar. The carbon chains of the bitartrates are antiperiplanar, whereas the adjacent $O_{carbonyl}$–$O_{hydroxy}$ atoms are synperiplanar, as reported by others (Table 1, references in Table 2).

The hydrogen-bonding systems of the diastereoisomeric salts are also similar (Table 5): hydrogen bonds I and II are situated between the counterions, bonds III and IV between the bitartrates form an infinite chain along the *b* axis, and the strongest hydrogen bond (V) lies along the *c* axis to form a bitartrate chain of the head-to-tail type (see also Figures 1 and 2).

The atomic positions of the bitartrate chiral network and the $CH_3NH_2^+$ moiety are almost the same in both structures. The largest deviation using a model fitting program[8] is 0.25 Å

Table 1. Characteristic values for bitartrate structures from Cambridge Cyrstallographic Database (May 1984)[11]

Reference code	T_1	T_2	T_3	Space group	*a*	*b*	*c*	β
ADRTAR	0	180	187	$P2_12_12_1$	*7.402*[a]	28.202	6.995	90
AMHTAR	−2	187	179	$P2_12_12_1$	*7.648*	11.066	7.843	90
BIKZOK10	0	147	165	$P2_1$	9.033	16.106	*7.821*	92.58
BYPTAR10	−6	181	180	$P2_12_12_1$	29.552	*7.780*	7.766	90
CSHTAR10	−4	190	179	$P2_12_12_1$	8.076	11.621	*7.692*	90
ENGCOA	4	184	183	$P2_1$	12.351	7.671	10.189	110.71
ENGCOB	−3	180	195	$P2_1$	11.135	10.037	7.716	98.61
ENHTAR	−3	182	183	$P4_12_12$	*7.531*	*7.531*	30.065	90
ENOXCT20	5	183	177	$P2_12_12$	16.583	14.186	7.403	90
MEPTAR10	−3	180	186	$P2_1$	8.621	*7.074*	15.510	98.11
TARTAC23	5	185	184	$P2_1$	*7.733*	5.936	6.15	100.6
TRHTRT	4	31	180	$P2_1$	10.522	16.209	7.472	98.88
Present compounds								
RMERTA	6	−3	184	$P2_1$	14.039	6.899	*7.715*	91.4
SMERTA	0	−10	184	$P2_1$	14.377	6.854	*7.826*	93.9
RMERTA·$2H_2O$[7]	−14	187	185	$P2_1$	10.351	*7.047*	12.352	110.5
mean value	−1	180	182					

T_1 = torsion angle O(12)–C(13)–C(15)–O(16)[b]
T_2 = torsion angle O(21)–C(19)–C(17)–O(18)
T_3 = torsion angle C(13)–C(15)–C(17)–C(19)

[a] The unit-cell parameter determined by the head-to-tail-type hydrogen-bond is italicised. [b] See numbering in the Scheme, O(12) is arbitrarily chosen to be synperiplanar

Table 2. Bibilography of bitartrate structures

1 Adrenaline hydrogen (+)-tartrate (ADRTAR)
D. Carlstrom, *Acta Crystallogr.*, 1973, **B29**, 161
2 Ammonium hydrogen D-tartrate (AMHTAR)
A. J. Van Bommel and J. M. Bijvoet, *Acta Crystallogr.*, 1958, **11**, 61
3 (−)-(1*R*,5*R*,9*R*,13*S*)-*N*-(tetrahydrofurfuryl)normetazocine tartrate monohydrate (BIKZOK10)
O. M. Peeters, C. J. De Ranter, and N. M. Blaton, *Acta Crystallogr.*, 1982, **B38**, 3055
4 (+)-(−)-Methyl-3-benzoylpiperidine (*RR*)-(+)-bitartrate monohydrate (BYPTAR10)
G. Hite and J. R. Soares, *Acta Crystallogr.*, 1973, **B29**, 2935
5 Caesium hydrogen tartrate (CSHTAR10)
L. K. Templeton and D. H. Templeton, *Acta Crystallogr.*, 1978, **A34**, 368
6 (+)-*trans-O*-Ethylenediaminebis(glycinato)cobalt(III) hydrogen D-tartrate trihydrate (ENGCOA)
M. Kuramoto, *Bull. Chem. Soc. Jpn.*, 1979, **52**, 3702
7 (−)-*trans-O*-Ethylenediaminebis(glycinato)cobalt(III) hydrogen D-tartrate monohydrate (ENGCOB)
M. Kuramoto, *Bull. Chem. Soc. Jpn.*, 1979, **52**, 3702
8 Ethylenediammonium di(hydrogen tartrate) dihydrate (ENHTAR)
S. Perez, *Acta Crystallogr.*, 1977, **B33**, 1083
9 (−)-589-Oxalato-bis(ethylenediamine)cobalt(III) hydrogen D-tartrate dihydrate (ENOXCT20)
M. Kuramoto, Y. Kushi, and H. Yoneda, *Bull. Chem. Soc. Jpn.*, 1980, **53**, 125
10 (−)-(−)-1-Methyl-3-ethyl-3-benzoylpiperidine (*RR*)-(+)-bitartrate (MEPTAR10)
J. R. Ruble, G. Hite, and J. R. Soares, *Acta Crystallogr.*, 1976, **B32**, 136
11 (+)-(2*R*,3*R*)-tartaric acid (TARTAC23)
H. Hope and U. De la Camp, *Acta Crystallogr.*, 1972, **A28**, 201
12 (Glutamyl-α-lactam)histidinylproline tartrate monohydrate (TRHTRT)
K. Kamiya, M. Takamuto, Y. Wada, M. Fujino, and M. Nishikawa, *J. Chem. Soc., Chem. Commun.*, 1980, 438

Table 3. Crystallographic data

Data	SMERTA	RMERTA
Formula	$C_{10}H_{16}N^+·C_4H_5O_6^-$	$C_{10}H_{16}N^+·C_4H_5O_6^-$
M	299.33	299.33
a/Å	14.377(2)	14.039(4)
b/Å	6.854(1)	6.899(2)
c/Å	7.826(1)	7.715(2)
β/°	93.90(1)	91.39(2)
Space group	$P2_1$	$P2_1$
Z	2	2
D_c(g cm^{-3})	1.292(1)	1.331(1)
μ(Mo-K_α) (cm^{-1})	0.946	0.977
Number of reflections [$I > 3\sigma(I)$]	1 811	933
R	0.037	0.034
R_w	0.045	0.037

Table 4. Selected torsion angles (°)

N-Methylamphetamine	SMERTA	RMERTA
C(1)–N(2)–C(3)–C(4)	−77.7(4)	70.5(6)
C(1)–N(2)–C(3)–C(5)	47.3(4)	−54.7(5)
N(2)–C(3)–C(5)–C(6)	168.7(5)	−168.7(7)
C(3)–C(5)–C(6)–C(7)	93.4(5)	−94.1(7)
Bitartrate		
O(12)–C(13)–C(15)–O(16)	0.4(3)	5.9(5)
O(14)–C(13)–C(15)–C(17)	54.6(3)	59.1(5)
O(16)–C(15)–C(17)–O(18)	−69.7(3)	−69.7(5)
C(13)–C(15)–C(17)–C(19)	−176.1(4)	−175.7(6)
C(15)–C(17)–C(19)–O(21)	−135.6(4)	−127.7(6)
O(18)–C(17)–C(19)–O(21)	−10.3(3)	−2.6(5)

[O(20)]. Short (C)–H · · · O_{tart} contacts were found, too. They are listed in Table 6. If the (*S*)- and (*R*)-*N*-methylamphetamine hemitartrates are compared again, contacts 1—3 can be regarded as by-products of the strong hydrogen-bond network. Contacts 4 and 5 are arranged along the *a* axis (Figures 3 and 4). The first contact is again similar, for both H(8) and O(20) are in the vicinity of the pseudomirror plane defined by C(1), N(2), and C(3).

Table 5. Hydrogen bonds of SMERTA and RMERTA

No.	D–H ··· A	Symmetry	D ··· A (Å)	H ··· A (Å)	D–H ··· A (°)
I	N(2)–H(2A) ··· O(14)	1_{000}	SMERTA 2.836(5)	1.87(1)	171(2)
			RMERTA 2.781(6)	1.92(4)	157(3)
II	N(2)–H(2B) ··· O(12)	1_{010}	SMERTA 2.813(5)	1.86(3)	168(2)
			RMERTA 2.936(6)	1.99(5)	140(3)
III	O(16)–H(16) ··· O(18)	2_{0-12}	SMERTA 2.783(5)	1.93(3)	153(2)
			RMERTA 2.782(6)	2.04(5)	149(3)
IV	O(18)–H(18) ··· O(14)	2_{0-12}	SMERTA 2.726(5)	1.89(3)	151(2)
			RMERTA 2.694(6)	1.89(4)	139(3)
V	O(21)–H(21) ··· O(12)	1_{001}	SMERTA 2.550(5)	1.81(3)	161(2)
			RMERTA 2.538(6)	1.52(4)	168(3)

Symmetry codes: 1 x,y,z; 2 $-x,\frac{1}{2}+y,-z$

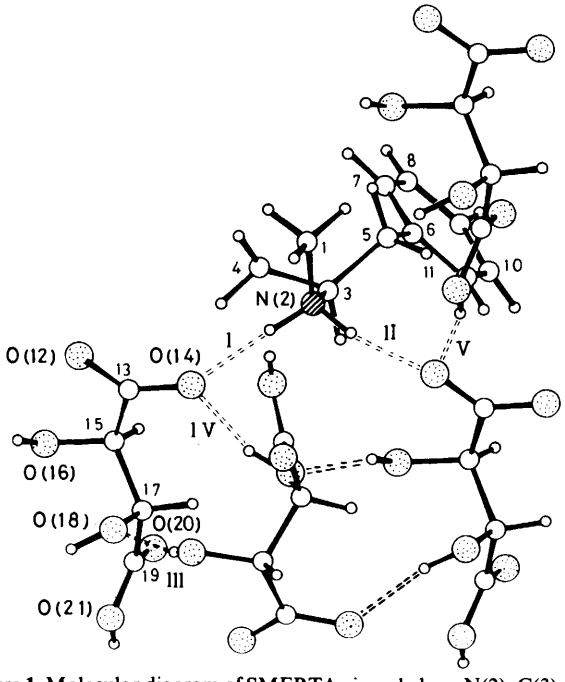

Figure 1. Molecular diagram of SMERTA viewed along N(2)–C(3) with hydrogen bonds I—V

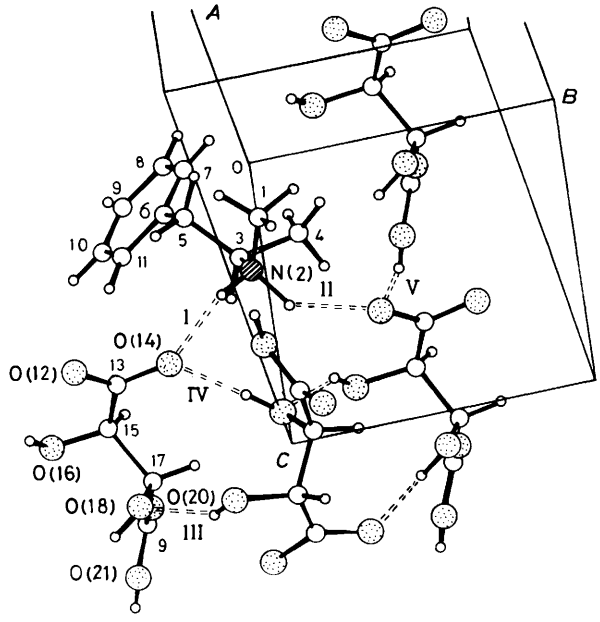

Figure 2. Molecular diagram of RMERTA viewed along N(2)–C(3) with hydrogen bonds I—V

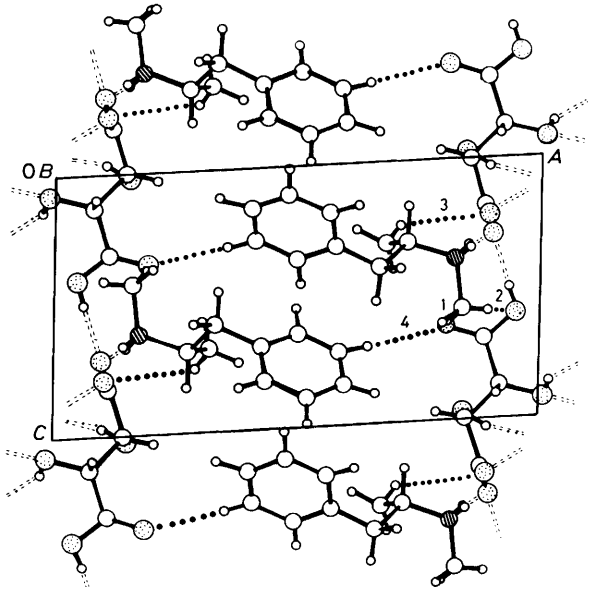

Figure 3. Packing arrangement of SMERTA viewed along *b*. Dotted lines represent C–H ··· O contacts 1—4

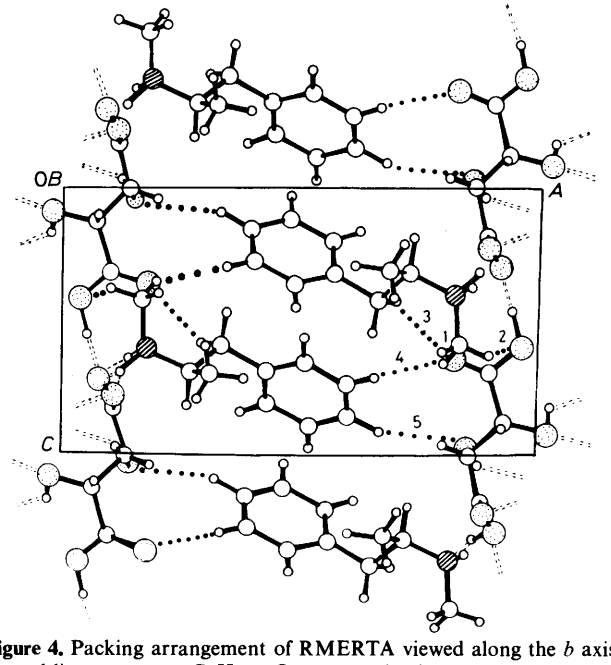

Figure 4. Packing arrangement of RMERTA viewed along the *b* axis. Dotted lines represent C–H ··· O contacts 1—5

Table 6. C–H · · · O contacts between cation and anion with C · · · O distance less than 3.6 Å

No.	D–H · · · A	Symmetry	D · · · A (Å)	H · · · A (Å)	D–H · · · A (°)
		RMERTA			
1	C(1)–H(1C) · · · O(20)	1_{00-1}	3.310(6)	2.54(4)	135(3)
2	C(1)–H(1B) · · · O(21)	2_{002}	3.330(6)	2.76(4)	118(3)
3	C(5)–H(5A) · · · O(20)	1_{00-1}	3.345(6)	2.58(4)	141(3)
4	C(8)–H(8) · · · O(20)	2_{102}	3.476(6)	2.54(4)	168(3)
5	C(9)–H(9) · · · O(16)	2_{102}	3.524(6)	2.58(5)	152(3)
		SMERTA			
1	C(1)–H(1A) · · · O(20)	1_{00-1}	3.334(5)	2.47(3)	146(2)
2	C(1)–H(1C) · · · O(21)	2_{002}	3.339(5)	2.67(3)	139(2)
3	C(4)–H(4B) · · · O(14)	1_{000}	3.351(5)	2.70(3)	124(2)
4	C(8)–H(8) · · · O(20)	2_{102}	3.389(5)	2.47(3)	158(2)
	C(9)–H(9) · · · O(16)	2_{102}	4.756(5)	3.87(4)	147(2)

In RMERTA an additional contact [C(9)–H(9) · · · O(16)] is also present, formed between atoms far from the pseudomirror plane. This additional contact along the *a* axis explains the shortening of this lattice parameter by 0.3 Å.

A recent paper by Taylor and Kennard provided crystallographic evidence of the existence of C–H · · · O contacts.[9] Although the H · · · O distances in our samples are only slightly shorter than the sum of the van der Waals radii (2.7 Å), since this is the most significant contact along one of the crystallographic directions, we suggest that these contacts may play an important role in enantiomer discrimination.

The fact that the number of second-order C–H · · · O interactions, taking into account all possible H · · · O contacts between the counter ions, is greater in RMERTA than in SMERTA means a more compact crystal structure (see Table 3), and therefore the RMERTA salt must be more stable and less soluble. The experimental data show that the solubility ratio SMERTA:RMERTA is *ca.* 25:1. The m.p. difference also proves that RMERTA is the more stable (Table 7).

Conclusions.—The experimental data support our hypothesis that the results of optical resolutions *via* diastereoisomeric salt formation are determined by weak second-order interactions.[2] It can also be seen in our model that the solubility and thermal behaviour differences between diastereoisomeric salts cannot be explained on the basis of differences in the strong interactions. The five unique hydrogen bonds involved in the salt bridge are equally available to both isomers, so the specific recognition process must involve some further binding–recognition site. In each bitartrate unit connected by very strong hydrogen bonds into an infinite chain, there are two acceptor-type chiral recognition 'forks': one is O(14)–C–C–C–O(18) binding the neighbouring bitartrate along the two-fold screw axis, while the other is O(20)–C–C–C–O(16), which is in C–H · · · O contact with the aromatic part of the base. These latter contacts (4 and 5 in Figure 5) distinguish between the *R*- and the *S*-base. (*RR*)-tartaric acid preferentially crystallises with the *R*-base. Preliminary studies on other *N*-methylamphetamine derivatives show that this is true for other *C*- and *N*-alkyl substituted derivatives, but substitution at the *meta*- and *para*-positions of the aromatic ring may have a profound effect on the preferred resolution. The good chiral ability of tartaric acid, frequently observed in nature, is due to its specific structure.

During diastereoisomeric bitartrate formation, the sterically determined tartrate chains linked by strong hydrogen bonds 'recognize' (still in solution) the *R*- and *S*-base isomers approaching them by Coulombic attraction. Hence, the resolution process is a simple model for the reactions playing important roles in biological systems. The ordered bitartrate chains, as hollow structural receptors react with that substrate (from the molecules to be resolved) whose size allows it to be fitted to the given steric structure of the chains, or for which only slight conformational changes are required for the most favourable and stereospecific binding. The preferred 'biological answer' is the crystallisation of one of the diastereoisomeric salts.

Table 7. Physicochemical data on diastereoisomeric salts

	SMERTA	RMERTA
M.p. (°C)	115 ± 1	164 ± 1
Enthalpy of fusion (kJ mol^{-1})	70.0* ± 2.1	48.8 ± 1.5
Solubility in ethanol (20 °C, g per 100 g solvent)	4.10 ± 2	0.16 ± 3

* Decomposition process accompanies the melting of SMERTA

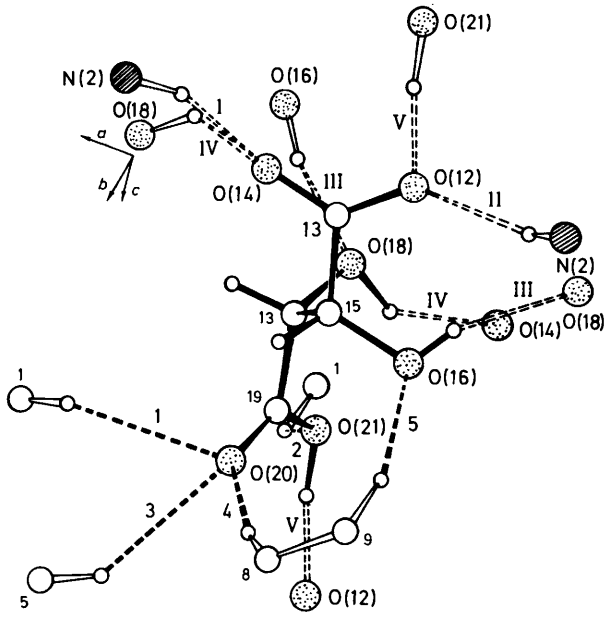

Figure 5. Hydrogen-bonding (I—V) and C–H · · · O contacts 1—5 around a bitartrate anion for RMERTA

Experimental

Optical Resolution of (±)-N-*Methylamphetamine.*[10]—Racemic base (3 g, 0.02 mol) was dissolved in absolute ethanol (8 ml). To this clear solution, a solution of tartaric acid (3 g) in absolute ethanol (15 ml) was added dropwise with continuous stirring. The precipitation of diastereoisomeric salt mixture started immediately. The mixture was stirred at 5 °C for 72 h, and the crystalline mass was then filtered off and recrystallised from absolute ethanol, $[\alpha]_D^{20}$ +4.77° (*c* 5, water), m.p. 163—164 °C for (*R*)-(−)-*N*-methylamphetamine (*RR*)-tartrate (RMERTA). The mother liquor was concentrated to dryness. The residue was recrystallised from ethanol, until the optical rotation was unchanged $[\alpha]_D^{20}$ +22.1° (*c* 5, water), m.p. 114—115 °C for (*S*)-(+)-*N*-methylamphetamine (*RR*)-tartrate (SMERTA).

Table 8. Fractional co-ordinates of SMERTA; estimated standard deviations are in parentheses

Atom	*x*	*y*	*z*
C(1)	0.160 6(1)	−0.008 8(0)	0.426 2(3)
N(2)	0.175 0(1)	0.000 0(4)	0.615 9(2)
C(3)	0.275 1(1)	0.009 8(4)	0.688 6(3)
C(4)	0.318 1(2)	−0.190 5(5)	0.683 6(4)
C(5)	0.329 0(1)	0.184 0(5)	0.593 2(3)
C(6)	0.423 2(2)	0.206 6(4)	0.683 9(3)
C(7)	0.501 8(2)	0.108 1(5)	0.639 5(3)
C(8)	0.588 1(2)	0.147 3(8)	0.721 0(4)
C(9)	0.596 9(2)	0.289 5(7)	0.843 4(5)
C(10)	0.520 8(2)	0.390 2(6)	0.888 3(4)
C(11)	0.434 4(2)	0.347 5(5)	0.810 8(4)
O(12)	0.098 4(1)	−0.641 8(3)	0.711 4(1)
C(13)	0.114 2(1)	−0.506 4(4)	0.818 1(2)
O(14)	0.105 5(1)	−0.329 3(3)	0.785 9(2)
C(15)	0.145 9(1)	−0.561 3(3)	1.002 5(2)
O(16)	0.154 2(1)	−0.765 2(2)	1.029 5(2)
C(17)	0.079 8(1)	−0.467 1(3)	1.122 6(2)
O(18)	−0.013 4(1)	−0.524 8(2)	1.078 1(1)
C(19)	0.112 0(1)	−0.505 3(4)	1.308 5(2)
O(20)	0.191 9(1)	−0.484 1(3)	1.359 7(2)
O(21)	0.044 9(1)	−0.556 0(3)	1.403 3(1)
H(1A)	0.190(1)	−0.125(4)	0.377(3)
H(1B)	0.200(1)	0.089(4)	0.371(3)
H(1C)	0.103(1)	−0.030(5)	0.411(3)
H(2A)	0.146(1)	−0.114(4)	0.665(3)
H(2B)	0.144(1)	0.112(4)	0.660(3)
H(3)	0.272(1)	0.045(4)	0.823(3)
H(4A)	0.379(1)	−0.198(4)	0.741(3)
H(4B)	0.290(1)	−0.291(5)	0.754(3)
H(4C)	0.305(1)	−0.245(5)	0.582(3)
H(5A)	0.337(1)	0.126(4)	0.467(2)
H(5B)	0.288(1)	0.286(4)	0.589(3)
H(7)	0.495(1)	0.011(5)	0.548(2)
H(8)	0.644(1)	0.074(4)	0.701(3)
H(9)	0.663(1)	0.326(5)	0.887(3)
H(10)	0.552(1)	0.464(6)	0.988(4)
H(11)	0.378(1)	0.419(4)	0.835(3)
H(15)	0.209(1)	−0.506(4)	1.033(2)
H(16)	0.104(1)	−0.821(4)	0.967(2)
H(17)	0.084(1)	−0.327(4)	1.100(2)
H(18)	−0.024(1)	−0.642(5)	1.129(3)
H(21)	0.063(1)	−0.556(4)	1.498(2)

Table 9. Fractional co-ordinates of RMERTA; estimated standard deviations are in parentheses

Atom	*x*	*y*	*z*
C(1)	0.171 5(2)	0.044 9(0)	0.414 4(5)
N(2)	0.176 8(2)	0.000 0(5)	0.603 0(3)
C(3)	0.276 5(2)	−0.007 9(6)	0.683 8(4)
C(4)	0.317 4(3)	0.195 0(6)	0.691 9(5)
C(5)	0.338 5(3)	−0.151 1(6)	0.584 3(5)
C(6)	0.431 1(2)	−0.192 7(6)	0.680 4(5)
C(7)	0.511 7(3)	−0.089 0(6)	0.644 9(5)
C(8)	0.597 1(3)	−0.132 2(8)	0.730 7(5)
C(9)	0.603 7(3)	−0.277 5(7)	0.848 7(5)
C(10)	0.523 9(3)	−0.380 7(7)	0.885 5(6)
C(11)	0.437 2(3)	−0.340 4(6)	0.802 1(5)
O(12)	0.092 1(1)	−0.635 0(4)	0.719 8(3)
C(13)	0.112 7(2)	−0.496 4(5)	0.820 5(4)
O(14)	0.109 0(2)	−0.321 5(4)	0.779 0(3)
C(15)	0.141 8(2)	−0.540 9(5)	1.005 7(4)
O(16)	0.151 8(1)	−0.740 6(3)	1.042 3(3)
C(17)	0.072 3(2)	−0.445 5(5)	1.126 5(4)
O(18)	−0.021 2(1)	−0.508 9(3)	1.089 7(2)
C(19)	0.104 0(2)	−0.475 0(5)	1.314 5(4)
O(20)	0.183 2(1)	−0.430 9(4)	1.364 0(3)
O(21)	0.039 0(1)	−0.546 6(4)	1.413 1(2)
H(1A)	0.204(2)	0.176(6)	0.389(4)
H(1B)	0.106(2)	0.064(6)	0.373(4)
H(1C)	0.199(2)	−0.064(6)	0.349(4)
H(2A)	0.148(2)	−0.115(6)	0.631(4)
H(2B)	0.129(2)	0.090(7)	0.685(5)
H(3)	0.270(2)	−0.057(6)	0.809(4)
H(4A)	0.306(2)	0.277(8)	0.589(5)
H(4B)	0.290(3)	0.257(7)	0.789(5)
H(4C)	0.387(3)	0.189(7)	0.711(5)
H(5A)	0.300(2)	−0.261(6)	0.576(4)
H(5B)	0.349(2)	−0.098(6)	0.462(4)
H(7)	0.510(2)	0.008(6)	0.559(4)
H(8)	0.652(2)	−0.059(6)	0.704(5)
H(9)	0.668(3)	−0.304(8)	0.910(5)
H(10)	0.524(2)	−0.488(7)	0.970(5)
H(11)	0.382(2)	−0.409(6)	0.836(4)
H(15)	0.197(2)	−0.471(5)	1.040(4)
H(16)	0.123(2)	−0.807(6)	0.968(4)
H(17)	0.076(2)	−0.302(5)	1.106(3)
H(18)	−0.026(2)	−0.614(6)	1.171(4)
H(21)	0.056(2)	−0.567(6)	1.543(4)

Crystals of SMERTA and RMERTA were obtained from dry ethanol. Crystal data are listed in Table 3. Data were collected on an Enraf–Nonius CAD-4 diffractometer with monochromated Mo-K_α radiation at the Central Research Institute for Chemistry of the Hungarian Academy of Sciences, Budapest. The crystals of RMERTA were thin plates (0.02 mm) and, therefore, data collection was restricted up to $\theta = 25°$, while well developed crystals of SMERTA could be mounted allowing data collection up to $\theta = 30°$. Reflections with $I > 3\sigma(I)$ were used in the refinement in all cases. All calculations were carried out on a PDP 11/34 minicomputer by means of the Enraf–Nonius SDP program package, with local modifications. The structures were solved by direct methods. Full-matrix least-squares refinements were carried out with all non-hydrogen atoms anisotropic and with isotropic hydrogen atoms taken from difference Fourier calculations. Hydrogen-atom positions were refined in two cycles applying a damping factor of 0.5. The weighting scheme was $w = 1/[\sigma^2(F_o) + 0.01\ F_o^2]$. Atomic co-ordinates are given in Tables 8 and 9. Atomic co-ordinates given represent the absolute configurations based on the known chirality of tartaric acid. Bond lengths, bond angles, and anisotropic thermal parameters are listed in the Supplementary Publication No. SUP 56648 (7 pp.).*

Acknowledgements

We are grateful to the *X*-ray Laboratory at the Central Research Institute for Chemistry, Hungarian Academy of Sciences, Budapest, Hungary, for facilities, to Dr. G. Pokol, Department of General and Applied Chemistry, Technical University, Budapest, for d.s.c. investigations, and to the CHINOIN Pharmaceutical and Chemical Works for support.

References

1 E. Fogassy, A. Lopata, F. Faigl, F. Darvas, M. Ács, and L. Töke, *Tetrahedron Lett.*, 1980, **21**, 547.

* For details of Supplementary Publications see Introduction for Authors in *J. Chem. Soc., Perkin Trans. 2*, 1986, Issue 1.

2 E. Fogassy, F. Faigl, and M. Ács, *Tetrahedron*, 1985, **41**, 2837.
3 W. Birkmayer, P. Riederer, and L. Ambrozi, *Lancet*, 1977, 439.
4 S. Larsen, *Acta Crystallogr.*, 1975, **A31**, S168.
5 S. Larsen, *Acta Crystallogr.*, 1978, **A34**, S98.
6 M. Kuramoto, Y. Kushi, and H. Yoneda, *Bull. Chem. Soc. Jpn.*, 1980, **53**, 125.
7 K. Simon, Z. Ecsery, J. Rohonczy, E. Fogassy, M. Ács, and F. Faigl, *Acta Crystallogr.*, 1984, **A40**, C81.
8 L. G. Hoard, 'ABCLS: Least Squares Model Fitting Programme,' University of Michigan, Ann Arbor.
9 R. Taylor and O. Kennard, *J. Am. Chem. Soc.*, 1982, **104**, 5063.
10 M. Ács and E. Fogassy, *Per. Polytechn. Chem. Eng.*, 1977, **21**, 221.
11 F. H. Allen, S. Bellard, M. D. Brice, B. A. Cartwright, A. Doubleday, H. Higgs, T. Hummelink, B. G. Hummelink-Peters, O. Kennard, W. D. S. Motherwell, J. R. Rodgers, and D. G. Watson, *Acta Crystallogr.*, 1979, **B35**, 2331.

Received 17*th September* 1985; *Paper* 5/1649